

# ACCEPTED VERSION

David McInerney, Mark Thyer, Dmitri Kavetski, Bree Bennett, Julien Lerat, Matthew Gibbs, George Kuczera

**A simplified approach to produce probabilistic hydrological model predictions**

Environmental Modelling & Software, 2018; 109:306-314

Crown Copyright © 2018 Published by Elsevier Ltd. All rights reserved.

This manuscript version is made available under the CC-BY-NC-ND 4.0 license

<http://creativecommons.org/licenses/by-nc-nd/4.0/>

Final publication at <http://dx.doi.org/10.1016/j.envsoft.2018.07.001>

## PERMISSIONS

<https://www.elsevier.com/about/our-business/policies/sharing>

Accepted Manuscript

Authors can share their [accepted manuscript](#):

### Immediately

- via their non-commercial personal homepage or blog
- by updating a [preprint](#) in arXiv or RePEc with the [accepted manuscript](#)
- via their research institute or institutional repository for internal institutional uses or as part of an invitation-only research collaboration work-group
- directly by providing copies to their students or to research collaborators for their personal use
- for private scholarly sharing as part of an invitation-only work group on [commercial sites with which Elsevier has an agreement](#)

### After the embargo period

- via non-commercial hosting platforms such as their institutional repository
- via commercial sites with which Elsevier has an agreement

**In all cases [accepted manuscripts](#) should:**

- link to the formal publication via its DOI
- bear a CC-BY-NC-ND license – this is easy to do
- if aggregated with other manuscripts, for example in a repository or other site, be shared in alignment with our [hosting policy](#)
- not be added to or enhanced in any way to appear more like, or to substitute for, the published journal article

**23 March 2021**

<http://hdl.handle.net/2440/114209>

# A simplified approach to produce probabilistic hydrological model predictions

David McInerney<sup>(1)</sup>, Mark Thyer<sup>(1)</sup>, Dmitri Kavetski<sup>(1)</sup>,  
Bree Bennett<sup>(1)</sup>, Julien Lerat<sup>(2)</sup>, Matthew Gibbs<sup>(3)</sup> and George Kuczera<sup>(4)</sup>

(1) School of Civil, Environmental and Mining Engineering, University of Adelaide, SA, Australia

(2) Bureau of Meteorology, Canberra, ACT, Australia

(3) Department of Environment, Water and Natural Resources, Government of South Australia, Australia

(4) School of Engineering, University of Newcastle, Callaghan, NSW, Australia

## Abstract

Probabilistic predictions from hydrological models, including rainfall-runoff models, provide valuable information for water and environmental resource risk management. However, traditional “deterministic” usage of rainfall-runoff models remains prevalent in practical applications, in many cases because probabilistic predictions are perceived to be difficult to generate. This paper introduces a simplified approach for hydrological model inference and prediction that bridges the practical gap between “deterministic” and “probabilistic” techniques. This approach combines the Least Squares (LS) technique for calibrating hydrological model parameters with a simple method-of-moments (MoM) estimator of error model parameters (here, the variance and lag-1 autocorrelation of residual errors). A case study using two conceptual hydrological models shows that the LS-MoM approach achieves probabilistic predictions with similar predictive performance to classical maximum-likelihood and Bayesian approaches, but is simpler to implement using common hydrological software and has a lower computational cost. A public web-app to help users implement the simplified approach is available.

**Keywords:** probabilistic prediction, rainfall-runoff modelling, method of moments, maximum likelihood

## Highlights

- New simplified approach for producing probabilistic hydrological predictions
- Similar performance to maximum-likelihood approach, at lower computational cost
- Web-app available to facilitate uptake of probabilistic predictions

31 **Software availability**

32 **Product title:** Interactive Probabilistic Predictions

33 **Description:** Web application for implementing Stage 2 of the LS-MoM approach introduced in this  
34 study

35 **Developer:** David McInerney, Bree Bennett, Mark Thyer, Dmitri Kavetski

36 **Contact Address:** David McInerney, School of Civil, Environmental and Mining Engineering,  
37 University of Adelaide, SA, Australia

38 **Contact Email:** david.mcinerney@adelaide.edu.au

39 **Software Required:** Web browser supported by R Shiny Server (Google Chrome, Mozilla Firefox,  
40 Safari)

41 **Available Since:** September 2017

42 **Availability:** <http://www.probabilisticpredictions.org>

43

## 44 1. Introduction

45 Predictions from hydrological models, particularly rainfall-runoff models, provide essential inputs to the  
46 planning and operation of water resource systems (Loucks et al., 1981). Probabilistic inference and  
47 prediction approaches, where probability models are used to describe data and model uncertainty, are of  
48 particular interest to enable uncertainty quantification and risk assessment (Vogel, 2017). Probabilistic  
49 techniques are well-known in the hydrological research community and include method-of-moments  
50 (MoM), maximum-likelihood (ML) and Bayesian techniques (e.g., Salas, 1993, Martins and Stedinger,  
51 2000), with rainfall-runoff model applications typically employing Bayesian techniques (e.g., Kuczera,  
52 1983, Krzysztofowicz, 2002, Schoups and Vrugt, 2010, Smith et al., 2010, Li et al., 2016, McInerney et  
53 al., 2017, Kavetski, 2018). Maximum-likelihood and Bayesian techniques require the specification of a  
54 likelihood function, which in rainfall-runoff modelling is typically derived from a residual error model,  
55 such as the widely used independent Gaussian error model. In most cases, residual error models include  
56 calibrated parameters of their own, such as error variance, lag-1 autocorrelation, and so forth.

57 In contrast to the research literature, practical hydrological modelling applications tend to rely on  
58 “deterministic” approaches, e.g., where rainfall-runoff models are calibrated using goodness-of-fit  
59 objective functions and quantification of uncertainty in predictions is typically considered the domain  
60 of applied research (Vaze et al., 2012). Least Squares (LS) objective functions (e.g., the sum-of-squared-  
61 errors (SSE) and equivalent Nash-Sutcliffe efficiency (NSE)) are widely used in research and practice;  
62 they are computed directly or from transformed flows (Chapman, 1970, Chiew et al., 1993, Oudin et al.,  
63 2006, Pushpalatha et al., 2012). Many hydrological modelling and calibration platforms implement LS  
64 objective functions. For example, the popular calibration package PEST supports weighted SSE  
65 (Doherty, 2004), HEC-HMS (Scharffenberg et al., 2006), the Australian “eWater Source” (Welsh et al.,  
66 2013) and HBV Light (Seibert, 2005) support log-transformed SSE (often used to better capture low  
67 flows), the Hydromad R package (Andrews et al., 2011) allows for objective functions based on Box-  
68 Cox transformed flows, and the recent airGR R package (Coron et al., 2017) provides built-in log,  
69 square-root and inverse-transformed SSE objective functions. Some of these software packages have  
70 capabilities for estimating parameter uncertainty and its impact on predictions. For example, PEST  
71 supports linear/nonlinear parameter uncertainty analysis including the null space Monte Carlo method  
72 (Tonkin and Doherty, 2009), and Hydromad implements the DREAM MCMC approach of Vrugt et al.  
73 (2009) (<http://hydromad.catchment.org>; see Joseph and Guillaume (2013) for an application).

74 The statistical modelling needed to derive the likelihood function and estimate the error model  
75 parameters creates a perception that probabilistic prediction requires substantial additional effort. For

76 example, in the software packages listed above, it is (relatively) easy to implement new objective  
 77 functions, but non-trivial to incorporate calibrated error model parameters. This perception can delay the  
 78 uptake of probabilistic techniques, especially in practical applications. The motivation of this study is to  
 79 develop a simplified approach that produces high-quality probabilistic rainfall-runoff model predictions  
 80 at a minor additional effort beyond that required for traditional deterministic predictions.

81 The specific aims of this study are:

82 **Aim 1.** Develop a simplified “LS-MoM” approach to generating probabilistic hydrological predictions,  
 83 exploiting a combination of Least Squares (LS) and method-of-moments (MoM) approaches;

84 **Aim 2.** Empirically compare the LS-MoM, maximum-likelihood and Bayesian approaches in terms of  
 85 predictive performance and computational cost, in a case study using conceptual hydrological models;

86 **Aim 3.** Introduce a public web-app to help practitioners apply the LS-MoM approach.

87 The paper continues by outlining the likelihood-based framework in Section 2. The LS-MoM approach  
 88 is developed in Section 3. Section 4 describes the empirical case study methods, with results reported in  
 89 Section 5. Sections 6-7 discuss and summarize the key findings.

## 90 **2. Likelihood-based parameter inference**

### 91 **2.1. Theory**

92 A hydrological (rainfall-runoff) model,  $H$ , simulates streamflow  $\mathbf{Q}^{0_H} = \{Q_t^{0_H}, t = 1, \dots, T\}$  over a series of  
 93 time steps  $t$ , as a function of forcing data  $\mathbf{X}$ , hydrological model parameters  $\boldsymbol{\theta}_H$  and initial conditions  
 94  $\mathbf{S}_0$ ,

$$95 \quad \mathbf{Q}^{0_H} = H(\boldsymbol{\theta}_H; \mathbf{X}, \mathbf{S}_0) \quad (1)$$

96 To estimate  $\boldsymbol{\theta}_H$  from observed streamflow data  $\tilde{\mathbf{Q}} = \{\tilde{Q}_t, t = 1, \dots, T\}$  and observed forcing data  $\tilde{\mathbf{X}}$  using  
 97 a maximum-likelihood approach, a likelihood function  $\mathcal{L}(\boldsymbol{\theta}_H; \tilde{\mathbf{Q}})$  should be specified and maximized  
 98 with respect to  $\boldsymbol{\theta}_H$ . The likelihood function is derived from an assumed probability model of observed  
 99 data,  $\mathcal{L}(\boldsymbol{\theta}_H; \tilde{\mathbf{Q}}) = p(\tilde{\mathbf{Q}} | \boldsymbol{\theta}_H, \tilde{\mathbf{X}})$ , e.g., by considering the probability distribution of residual errors  
 100 assumed to describe the combined contributions of all sources of predictive error (Renard et al., 2011).  
 101 Residual errors of hydrological model are typically heteroscedastic (larger errors in larger flows) and  
 102 persistent (similar errors several time steps in a row) (e.g., Sorooshian and Dracup, 1980). In many cases,

103 error heteroscedasticity is represented using streamflow transformations (e.g., logarithmic or Box-Cox),  
 104 and error persistence is represented using an autoregressive lag-1, AR(1), model (e.g., Sorooshian and  
 105 Dracup, 1980, Evin et al., 2014). Under these assumptions, and ignoring terms at  $t=1$ , the (approximate)  
 106 likelihood is

$$107 \quad \mathcal{L}_F(\boldsymbol{\theta}_H, \boldsymbol{\theta}_Z, \boldsymbol{\theta}_\varepsilon; \tilde{\mathbf{Q}}) = p(\tilde{\mathbf{Q}} | \boldsymbol{\theta}_H, \boldsymbol{\theta}_Z, \boldsymbol{\theta}_\varepsilon, \tilde{\mathbf{X}}) = \prod_{t=2}^T Z'(\tilde{Q}_t; \boldsymbol{\theta}_Z) f_N(y_t(\boldsymbol{\theta}_H, \boldsymbol{\theta}_Z, \phi; \tilde{\mathbf{Q}}, \tilde{\mathbf{X}}); 0, \sigma_y^2) \quad (2)$$

108 The terms in equation (2) are as follows:

109 1)  $Z(Q)$  is the streamflow transformation used to describe error heteroscedasticity, and  $Z' = dZ / dQ$  is  
 110 its Jacobian. Here we employ the ubiquitous Box-Cox transformation (Box and Cox, 1964),

$$111 \quad Z(Q; \lambda, A) = \begin{cases} \frac{(Q+A)^\lambda - 1}{\lambda} & \text{if } \lambda \neq 0 \\ \log(Q+A) & \text{otherwise} \end{cases} \quad (3)$$

112 where  $\lambda$  and  $A$  are transformation parameters, grouped into  $\boldsymbol{\theta}_Z$  in equation (2). When  $A=0$ , the Box-  
 113 Cox transformation with  $\lambda=0, 0.5$ , and  $-1$  is equivalent to the log, square-root and inverse  
 114 transformations respectively.

115 The offset  $A$  can be non-dimensionalized by a typical streamflow magnitude, such as the mean  
 116 observed flow,

$$117 \quad A^* = A / \text{mean}(\tilde{\mathbf{Q}}) \quad (4)$$

118 2) The quantity  $y_t$  is the “error innovation” at time step  $t$ , defined from a zero-mean homoscedastic  
 119 Gaussian AR(1) model of residuals of transformed streamflows,

$$120 \quad \eta_t = Z(\tilde{Q}_t; \boldsymbol{\theta}_Z) - Z(Q_t^{0_H}; \boldsymbol{\theta}_Z) \quad (5)$$

$$121 \quad y_t = \eta_t - \phi_\eta \eta_{t-1} \quad (6)$$

$$122 \quad y_t \sim N(0, \sigma_y) \quad (7)$$

123 where  $N(\mu, \sigma)$  denotes the Gaussian distribution with mean  $\mu$  and variance  $\sigma^2$ , and probability density  
 124 function (pdf)  $f_N(x; \mu, \sigma^2)$ . The residual error model in equations (3)-(7) has parameters  $\boldsymbol{\theta}_\varepsilon = \{\phi_\eta, \sigma_y\}$ ,  
 125 where  $\phi_\eta$  is the lag-1 autoregressive parameter and  $\sigma_y$  is the standard deviation.

## 126 **2.2. Two-stage post-processor implementation**

127 A two-stage post-processing (PP) approach for parameter estimation is employed:

128 **Stage 1:** Calibrate hydrological and transformation parameters,  $\theta_H$  and  $\theta_Z$ , neglecting error  
 129 autocorrelation, i.e., maximizing the likelihood in equation (2) while fixing  $\phi_\eta = 0$ . The parameter  $\sigma_y$   
 130 is also calibrated, but then discarded in Stage 2. The transformation parameter  $\lambda$  can be either fixed *a*  
 131 *priori* or calibrated (e.g., Wang et al., 2012, McInerney et al., 2017);

132 **Stage 2:** Calibrate error model parameters,  $\theta_\varepsilon = \{\phi_\eta, \sigma_y\}$ , by maximizing the likelihood in equation (2)  
 133 while keeping  $\theta_H$  and  $\theta_Z$  fixed at the values estimated in Stage 1. Stage 2 is computationally very fast  
 134 because it works solely with observed data and optimal streamflow predictions from Stage 1, and hence  
 135 does not require additional hydrological model runs.

136 The adopted PP approach is empirically more robust than joint calibration, because it avoids problematic  
 137 interactions between hydrological and error model parameters (see Evin et al., 2014, and Supplementary  
 138 Material Section S1). As both stages are implemented using maximum-likelihood, we will refer to this  
 139 approach as the ML-ML approach.

140 When parsimonious hydrological models such as GR4J (e.g., Perrin et al., 2003) are calibrated to long  
 141 observed time series using residual error models such as those in Section 4, the contribution of  
 142 parametric uncertainty to total predictive uncertainty in streamflow is generally small (Kuczera et al.,  
 143 2006, Yang et al., 2007, Sun et al., 2017, Kavetski, 2018). For this reason, hydrological prediction and  
 144 forecasting applications tend to focus on residual errors and often ignore posterior parameter uncertainty  
 145 (e.g., England and Steinsland, 2014, McInerney et al., 2017). This is the strategy employed in this study,  
 146 where calibration is undertaken solely through optimization of the likelihood function. The suitability of  
 147 this approach is illustrated as described in Section 4.1, with limitations discussed in Section 6.4.

## 148 **3. Simplified approach for parameter inference**

149 The simplified approach has two stages that mimic those of the ML-ML approach:

150 **Stage 1:** Estimate hydrological model parameters  $\theta_H$  by Least Squares optimization (e.g., by  
 151 minimizing SSE). Transformation parameters  $\theta_Z$  (if any) must be fixed *a priori*;

152 **Stage 2:** Estimate error model parameters  $\theta_\varepsilon$  from the residuals  $\eta$  using the method-of-moments.

153 We will refer to this approach as LS-MoM; its respective equations are presented next.

### 154 **3.1. Stage 1**

155 When the transformation parameters  $\boldsymbol{\theta}_Z$  are fixed, the Jacobian term in equation (2) no longer depends  
 156 on any inferred quantity, and represents a proportionality constant. With the additional assumption that  
 157  $\boldsymbol{\eta}$  is uncorrelated (UC),  $\phi_\eta = 0$ , equation (2) reduces to

$$158 \quad \mathcal{L}_{UC}(\boldsymbol{\theta}_H, \sigma_\eta; \tilde{\mathbf{Q}}, \boldsymbol{\theta}_Z) \propto \prod_{t=1}^T f_N(\eta_t(\boldsymbol{\theta}_H, \boldsymbol{\theta}_Z; \tilde{\mathbf{Q}}_t, \tilde{\mathbf{X}}_{1:t}) | 0, \sigma_\eta^2) \quad (8)$$

159 where  $\sigma_\eta$  is the standard deviation of  $\boldsymbol{\eta}$  (McInerney et al., 2017).

160 Expanding  $f_N(x; \mu, \sigma^2)$  and taking logarithms, equation (8) can be re-written as

$$161 \quad \log \mathcal{L}_{UC}(\boldsymbol{\theta}_H, \sigma_\eta; \tilde{\mathbf{Q}}, \boldsymbol{\theta}_Z) = -\Psi_1(\sigma_\eta) - \Psi_2(\sigma_\eta) \Phi_{SSE}(\boldsymbol{\theta}_H; \tilde{\mathbf{Q}}, \tilde{\mathbf{X}}_{1:t}, \boldsymbol{\theta}_Z) + \text{const} \quad (9)$$

162 where  $\Psi_1 = T \ln(\sigma_\eta^2) / 2$  and  $\Psi_2(\sigma_\eta) = 1 / 2\sigma_\eta^2$  are functions solely of  $\sigma_\eta$ , and

$$163 \quad \Phi_{SSE}(\boldsymbol{\theta}_H; \cdot) = \sum_{t=1}^T \eta_t(\boldsymbol{\theta}_H; \cdot)^2 \quad (10)$$

164 is the sum of squared errors (SSE) of transformed flows, viewed solely as a function of  $\boldsymbol{\theta}_H$ .

165 Noting that  $\Psi_2 > 0$ , the hydrological parameter values  $\boldsymbol{\theta}_H$  that maximise  $\log \mathcal{L}_{UC}$  (and hence  $\mathcal{L}_{UC}$ ) are  
 166 the same ones that minimize  $\Phi_{SSE}$ . This equivalence is verified algebraically in Supplementary Material  
 167 Section S2, and is well-known in the statistical literature (e.g., Charnes et al., 1976).

168 In other words, under the assumptions of uncorrelated Gaussian residuals and provided the  
 169 transformation parameters are fixed, Stage 1 of the ML-ML approach can proceed through Least Squares  
 170 optimization of transformed flows. Table 1 provides the correspondence between common objective  
 171 functions and the SSE applied to Box-Cox transformed flows.

172 Note that, given the reduction in the number of optimized quantities in Stage 1 – which is the only stage  
 173 that requires running the hydrological model – it can be expected that LS-MoM is computationally  
 174 cheaper than ML-ML for a given optimization algorithm.

175 Table 1. Correspondence between common objective functions used in the hydrological literature and  
 176 Box-Cox transformation parameters applied to SSE.

Objective function	Transformation parameters	References
Sum of squared errors (SSE) of untransformed flows Root mean squared error (RMSE) Nash Sutcliffe Efficiency (NSE)	$\lambda = 1$ and $A^* = 0$	Servat and Dezetter (1991), Gan et al. (1997), Oudin et al. (2006), Kumar et al. (2010)
NSE of square root transformed flows	$\lambda = 0.5$ and $A^* = 0$	Chapman (1970), Chiew et al. (1993), Ye et al. (1998), Perrin et al. (2003), Oudin et al. (2006), Pushpalatha et al. (2012)
NSE of log transformed flows	$\lambda = 0$ and $A^* = 0$	Dawdy and Lichty (1968), Chapman (1970), Oudin et al. (2006), Kumar et al. (2010)
Likelihood function based on log transformed flow with non-zero offset	$\lambda = 0$ and $A^* \neq 0$	Bates and Campbell (2001), Smith et al. (2010)

177

### 178 3.2. Stage 2

179 Given estimated values  $\hat{\theta}_H$  from Stage 1 and fixed values of  $\theta_Z$ , the estimated residuals  $\hat{\eta}$  in equation  
 180 (5) are themselves fixed. The method-of-moments can then be used to estimate the error model  
 181 parameters  $\hat{\theta}_\varepsilon$  from sample statistics of  $\hat{\eta}$ .

182 The lag-1 autoregressive parameter  $\hat{\phi}_\eta$  is estimated as the sample lag-1 autocorrelation coefficient

$$183 \quad \hat{\phi}_\eta = \text{acorr}_{t=1}[\hat{\eta}] = \frac{1}{(T-1) s_{\hat{\eta}}^2} \sum_{t=2}^T (\hat{\eta}_t - m_{\hat{\eta}})(\hat{\eta}_{t-1} - m_{\hat{\eta}}) \quad (11)$$

184 where  $m_{\hat{\eta}} = \text{mean}[\hat{\eta}]$  and  $s_{\hat{\eta}}^2 = \text{var}[\hat{\eta}]$  denote, respectively, the sample mean and variance of  $\hat{\eta}$ .

185 The innovation variance  $\hat{\sigma}_y^2$  is estimated from the well-known relationship between conditional and  
 186 marginal variances of an AR(1) process (Box and Jenkins, 1970),

$$187 \quad \hat{\sigma}_\eta^2 = s_{\hat{\eta}}^2 = \text{var}[\hat{\eta}] = \frac{1}{T-1} \sum_{t=1}^T (\hat{\eta}_t - m_{\hat{\eta}})^2 \quad (12)$$

$$188 \quad \hat{\sigma}_y^2 = \hat{\sigma}_\eta^2 (1 - \hat{\phi}_\eta^2) \quad (13)$$

189 Once again, no additional hydrological model runs are required in Stage 2.

## 190 **4. Case study methods**

### 191 **4.1. Experiments and residual error schemes**

192 The objective of the case study is to establish if the simple LS-MoM approach (described in Section 3)  
 193 is competitive with the more complex ML-ML approach (described in Section 2.2) in hydrological  
 194 modelling applications. This comparison is carried out for the Box-Cox error models recommended by  
 195 McInerney et al. (2017), as follows:

- 196 1) Benchmarking of the LS-MoM approach against a “well-performing” ML-ML approach:
  - 197 a) For the residual error schemes recommended by McInerney et al. (2017), namely the Log ( $\lambda = 0$ )  
 198 ), BC0.2 ( $\lambda = 0.2$ ) and BC0.5 ( $\lambda = 0.5$ ) schemes in perennial catchments, and the BC0.2 and  
 199 BC0.5 schemes in ephemeral/low-flow catchments, we compare LS-MoM with fixed  $A^* = 0$   
 200 against the ML-ML approach with inferred  $A^*$  (Section 2.2). The value  $A^* = 0$  is of particular  
 201 interest in the LS-MoM approach because it provides the closest correspondence to common  
 202 objective functions (Table 1);
  - 203 b) When applying the Log scheme in ephemeral/low-flow catchments, ML-ML with inferred  $A^*$   
 204 performs poorly (McInerney et al., 2017), and LS-MoM with  $A^* = 0$  is not applicable. Hence,  
 205 in these scenarios, we set  $A^* = 10^{-1}$  in both the ML-ML and LS-MoM approaches;
- 206 2) Analysis of the LS-MoM approach with  $A^* = 0$ ,  $10^{-4}$  and  $10^{-1}$  (with  $A^* = 0$  excluded when using  
 207 the Log scheme in ephemeral/low-flow catchments). This experiment establishes the impact of the  
 208 offset, which must be specified *a priori* in the LS-MoM approach and could potentially impact on  
 209 calibration and prediction.

210 Given that the LS-MoM and ML-ML approaches compared in this work are set to ignore parameter  
 211 uncertainty, the contribution of parameter uncertainty to total predictive uncertainty in streamflow is  
 212 evaluated by comparing LS-MoM and ML-ML to two Bayesian setups, namely to a full Bayesian  
 213 approach where  $\theta_H$  and  $\theta_Z$  are inferred jointly, and to a Bayesian implementation of Stage 1 from  
 214 Section 2.2. The details of this comparison are reported in Supplementary Material Section S1.

### 215 **4.2. Hydrological data and models**

216 The case study setup from McInerney et al. (2017) is used, with 11 Australian catchments  
 217 (<http://www.bom.gov.au/water/hrs>) and 12 US catchments (Duan et al., 2006). For modelling purposes,

218 catchments are classified into two types: 11 catchments where the minimum observed flow is below 2%  
219 of the mean observed flow are referred to as “ephemeral/low-flow”; the remaining 12 catchments are  
220 termed “perennial” (see Supplementary Material Table S1 for details of the catchments). This  
221 classification was found to correlate better with probabilistic model performance than an earlier  
222 classification based on the proportion of zero flow days (McInerney et al., 2017), and is not intended as  
223 a classification from a hydrological process perspective.

224 Two conceptual rainfall-runoff models, GR4J (Perrin et al., 2003) and HBV (Bergström, 1995) are used.  
225 A cross-validation framework is implemented over a 10-year period (McInerney et al., 2017, Table 5)  
226 and used to produce a concatenated 10-year series of daily streamflow predictions. Predictive  
227 distributions are computed as described in Appendix A. Parameter optima are obtained from 100 quasi-  
228 Newton optimizations (Kavetski and Clark, 2010). The offset  $A^*$  is given a lower bound of  $10^{-7}$  to avoid  
229 the Jacobian in equation (2) becoming undefined for  $\tilde{Q}_t = 0$ ; all other bounds are taken from McInerney  
230 et al. (2017). “Typical” parameter values are obtained from a single calibration over the entire 10-year  
231 period.

### 232 **4.3. Evaluation criteria**

233 *Predictive performance* is assessed in terms of reliability, precision and bias, using the metrics from  
234 McInerney et al. (2017) (see Supplementary Material Section S4 for details). Reliability describes the  
235 degree of statistical consistency of predictive distributions and observations; precision refers to the width  
236 of predictive distributions; bias measures overall water balance errors. In all metrics, lower values  
237 indicate better performance.

238 *Estimates of parameters*  $A^*$ ,  $\phi_\eta$  and  $\sigma_y$  from the LS-MoM and ML-ML approaches are compared,  
239 including a check of how often the inferred  $A^*$  lies within machine precision of its lower bound.

240 *Computational cost* is quantified by the number of objective function evaluations (equivalent to the  
241 number of hydrological model calls), averaged over 100 independent optimizations, required for  
242 parameter optimization in Stage 1. This stage dominates the total cost in all schemes, because each  
243 objective function call in Stage 1 requires running the hydrological model; the cost of a *single* objective  
244 function evaluation in Stage 1 is essentially the same in all schemes.

245

## 246 5. Results

247 Figure 1 shows the predictive performance of all approaches. To facilitate comparison, Figure 2 shows  
 248 the distribution of differences in metric values against a baseline approach. The baseline is taken as LS-  
 249 MoM with  $A^* = 0$  in all scenarios except for the use of the Log scheme in ephemeral/low-flow  
 250 catchments, where  $A^* = 0$  is not applicable and the baseline is hence LS-MoM with  $A^* = 10^{-1}$ .

### 251 5.1. Comparison of LS-MoM and ML-ML approaches

252 Figure 1 shows that the LS-MoM approach with  $A^* = 0$  (red) has similar performance to the ML-ML  
 253 approach (dark blue), for most residual error schemes, catchments and metrics (excepting the Log  
 254 scheme applied in ephemeral/low-flow catchments). In most cases, performance metrics vary by about  
 255  $\pm 0.01$  (Figure 2). Even the largest difference between LS-MoM and ML-ML approaches, in the  
 256 precision of the BC0.2 scheme in ephemeral/low-flow catchments (Figure 2d, LS-MoM approach is  
 257 better by a median value  $\approx 0.02$ ), is much smaller than the differences between BC0.2 vs BC0.5 schemes  
 258 (median differences of  $\approx 0.11$  and  $\approx 0.08$  for LS-MoM and ML-ML approaches respectively).

259 The values of the offset and error model parameters in the two approaches are also similar. In the ML-  
 260 ML approach, the inferred value of  $A^*$  is at its lower bound of  $10^{-7}$  in 114 of 116 scenarios (excluding  
 261 Log in ephemeral/low-flow catchments), effectively matching the value  $A^* = 0$  used in the LS-MoM  
 262 approach. The values of error model parameters  $\phi_\eta$  and  $\sigma_y$  estimated using the two approaches differ  
 263 by less than 1%.

264 In ephemeral/low-flow catchments, the Log scheme with inferred offset  $A^*$  yields poor precision and  
 265 large biases (Figure 1d,f; see also McInerney et al. (2017)). Figure 1 shows that fixing the offset  $A^*$  to  
 266 a larger value of  $10^{-1}$  is highly beneficial, making the Log scheme competitive with the BC0.2 and  
 267 BC0.5 schemes; importantly ML-ML and LS-MoM approaches once again perform very similarly.

### 268 5.2. Sensitivity of LS-MoM approach to the offset parameter

269 The impact of the offset  $A^*$  on the LS-MoM approach is shown in Figures 1 and 2 for fixed values of  
 270  $A^* = 0$  (red),  $A^* = 10^{-4}$  (green) and  $A^* = 10^{-1}$  (cyan).

271

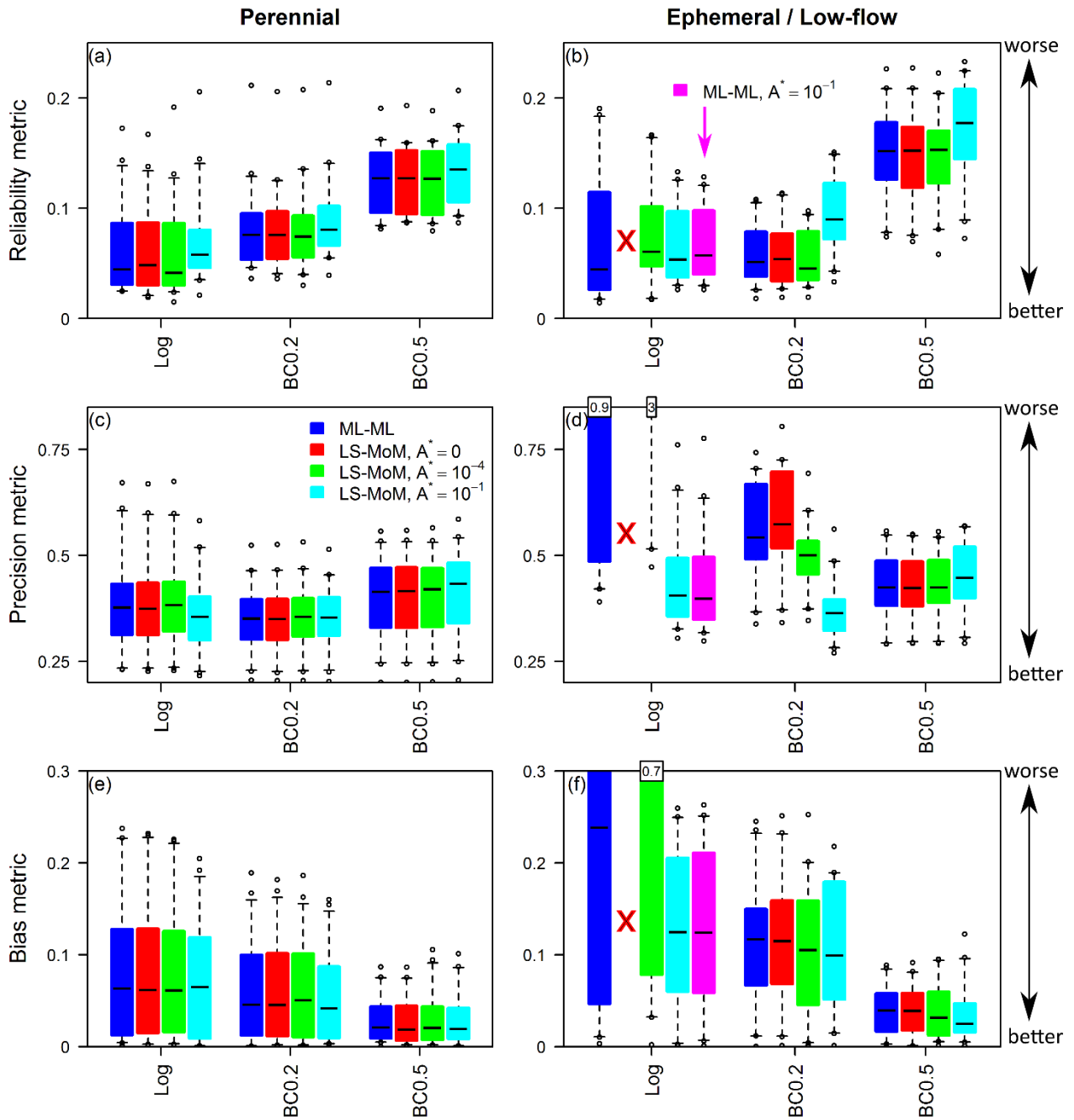


Figure 1: Predictive performance metrics of the LS-MoM approach with fixed  $A^* \in \{0, 10^{-4}, 10^{-1}\}$  and the ML-ML approach with inferred  $A^*$ . The whiskers represent 90% probability limits computed over the 23 case study catchments. Results of applying the Log scheme in ephemeral/low-flow catchments are presented with modifications: (i) LS-MoM with  $A^* = 0$  is not applicable (marked by red X), (ii) ML-ML with  $A^* = 10^{-1}$  is included because ML-ML with fitted  $A^*$  performs very poorly.

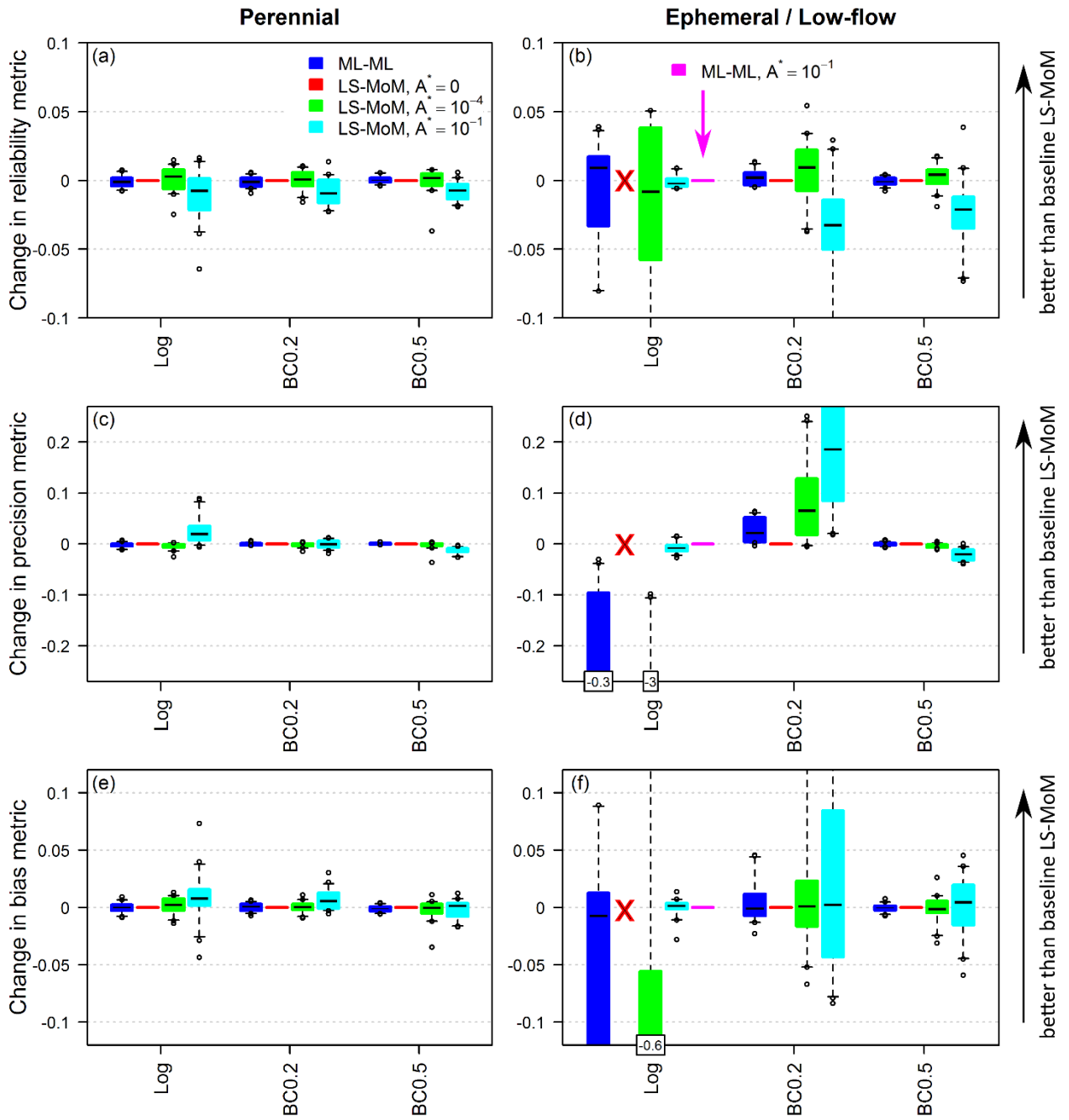


Figure 2: Difference in predictive performance metrics of the LS-MoM and ML-ML approaches in Figure 1. The baseline is given by the LS-MoM approach with  $A^* = 0$ , except for applications of the Log scheme in ephemeral/low-flow catchments, where the baseline is LS-MoM with  $A^* = 10^{-1}$ . Positive differences indicate schemes with better performance than the baseline LS-MoM approach.

274 In perennial catchments, all three values of  $A^*$  lead to similar predictive performance, with the largest  
275 changes occurring when  $A^* = 10^{-1}$ . For example, increasing  $A^*$  from 0 to  $10^{-1}$  worsens reliability in all  
276 schemes (Figure 2a, median change  $\approx 0.01$ ). However, this difference is much smaller than differences  
277 between the Log and BC0.5 schemes (Log scheme is better by a median value  $\approx 0.06$ ).

278 In ephemeral/low-flow catchments, the offset parameter plays a bigger role. The impact is most evident  
279 in the Log scheme, where  $A^* = 0$  is not applicable and increasing  $A^*$  from  $10^{-4}$  to  $10^{-1}$  substantially  
280 improves predictive performance (median precision tightens from  $\approx 3$  to  $\approx 0.4$ , and median bias reduces  
281 from  $\approx 0.7$  to  $\approx 0.12$ ). For the BC0.2 scheme, increasing  $A^*$  from 0 to  $10^{-4}$  improves reliability (Figure  
282 2b, median change  $\approx 0.01$ ) and precision (Figure 2d, median change  $\approx 0.07$ ). Increasing  $A^*$  to  $10^{-1}$   
283 worsens reliability (median increase  $\approx 0.03$ ), but further improves precision (median change  $\approx 0.18$ ). The  
284 offset value is less important in the BC0.5 scheme; the most noticeable difference is the worsening of  
285 reliability when  $A^* = 10^{-1}$  (median change  $\approx 0.02$ ).

### 286 **5.3. Effect of ignoring posterior parametric uncertainty**

287 Supplementary Material Section S1 reports the results of comparing LS-MoM and ML-ML against  
288 Bayesian implementations of the same residual error schemes. As shown in Supplementary Material  
289 Figure S1, the contribution of posterior parameter uncertainty to total predictive uncertainty in  
290 streamflow is small to negligible, and predictive performance metrics of LS-MoM are comparable to or  
291 better than the Bayesian approaches over the majority of catchments. These results are in line with  
292 theoretical expectations and previous empirical investigations (Kuczera et al., 2006, Yang et al., 2007,  
293 Sun et al., 2017, Kavetski, 2018, and others).

### 294 **5.4. Comparison of computational cost**

295 Figure 3 compares the number of objective function evaluations required for calibrating GR4J and HBV  
296 using the ML-ML approach with fitted  $A^*$  versus the LS-MoM approach with  $A^* = 0$  (excluding the  
297 Log scheme in ephemeral/low-flow catchments). When using GR4J, the LS-MoM approach more than  
298 halves the computational cost (based on the median value over all scenarios). When using HBV, the  
299 savings are slightly smaller, around 40%.

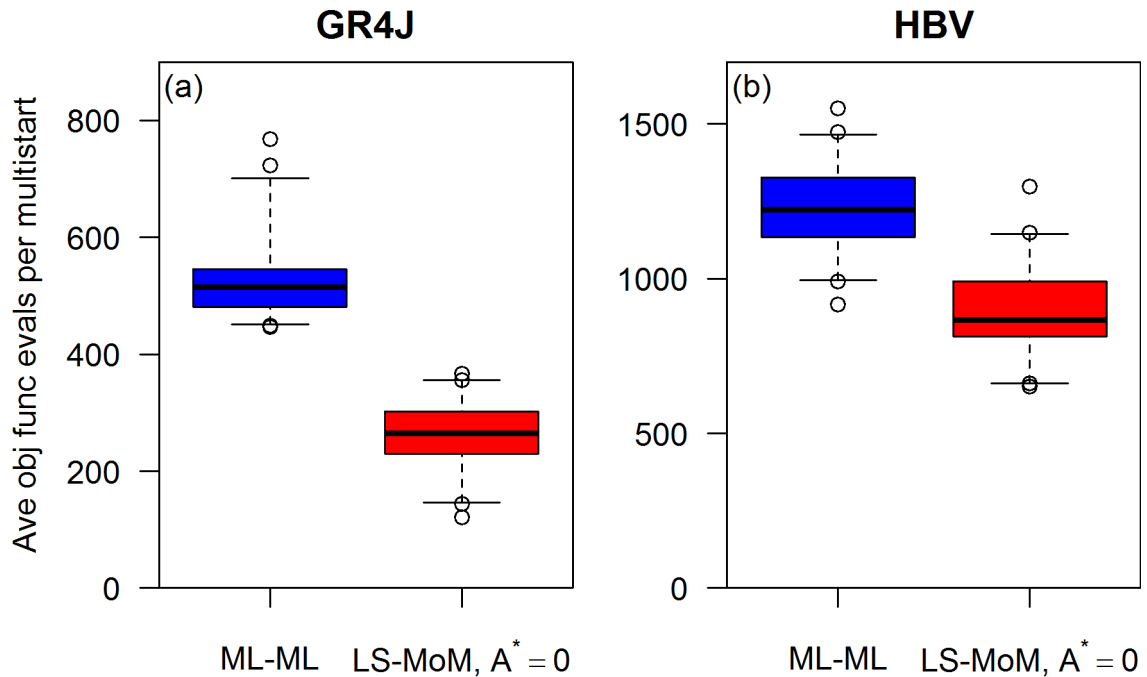


Figure 3: Computational cost of parameter optimization in Stage 1 of the ML-ML vs LS-MoM approaches. The number of objective function calls per invocation of a quasi-Newton optimizer is shown (averaged over 100 multistarts). Boxplots indicate results over all catchments and residual error schemes in Figures 1 and 2 (except for the Log scheme in ephemeral/low-flow catchments).

300

## 301 6. Discussion

### 302 6.1. Bona fides of the LS-MoM approach

303 The similar predictive performance of the LS-MoM and ML-ML approaches is explained by the  
 304 calibrated parameters having similar values. In particular, with the exception of the Log scheme applied  
 305 in ephemeral/low-flow catchments, the inferred  $A^*$  is generally close to 0, and hence to the fixed values  
 306 used in the LS-MoM approach with  $A^* = 0$ . Given similar values of  $A^*$ , the similarity of the two  
 307 approaches is expected from theory: the equivalence of Stage 1 hydrological parameter optima is shown  
 308 in Section 3.1, and the similarity of Stage 2 error parameter estimates reflects the general consistency of  
 309 maximum-likelihood and method-of-moments estimators of AR(1) process parameters.

310 The computational savings of the LS-MoM approach can be attributed to fewer estimated parameters,  
 311 as Stage 1 no longer calibrates  $A^*$  and  $\sigma_y$ . For example, in the case of GR4J, the dimension of the  
 312 search space is reduced by 33%. The cost savings might vary depending on the particular optimization  
 313 algorithm used, and further savings are likely if optimization algorithms adapted to LS-type objective

314 functions, such as the Levenberg-Marquardt method (e.g., Doherty, 2004), are exploited. Cost savings  
315 are expected to be even larger in comparison to a Bayesian approach using MCMC.

## 316 **6.2. Selection of offset value**

317 In the experiments reported here, as  $A^*$  increases, precision generally improves but reliability worsens.  
318 This trade-off is most evident in ephemeral/low-flow catchments, especially when the BC0.2 scheme is  
319 used, and is reminiscent of the trade-offs seen when changing the Box-Cox parameter  $\lambda$  (McInerney et  
320 al., 2017). Given that the LS-MoM approach requires all transformation parameters, including  $A^*$ , to be  
321 fixed *a priori*, we recommend starting with a value of  $A^* = 0$  and increasing it while monitoring relevant  
322 aspects of predictive performance. The exception is when the Log scheme is used in ephemeral/low-  
323 flow catchments, in which case a larger offset of  $A^* = 10^{-1}$  can improve the precision and reduce bias.

## 324 **6.3. Web-app implementing the LS-MoM approach**

325 A public-access web-app is provided at [www.algorithmik.org.au/apps/probabilisticPredictions](http://www.algorithmik.org.au/apps/probabilisticPredictions) to  
326 implement Stage 2 of the LS-MoM approach. The web-app assumes the user has already calibrated their  
327 hydrological model (Stage 1), using their preferred software and objective function (e.g., Table 1). The  
328 user uploads the observed and calibrated streamflow time series, and specifies  $\theta_z = \{\lambda, A^*\}$  used in  
329 Stage 1. The web-app then estimates the error model parameters  $\theta_\epsilon = \{\phi_\eta, \sigma_y\}$  (Stage 2) and generates  
330 probabilistic predictions. The web-app includes interactive display of probabilistic predictions and  
331 observed data time series, performance metrics and residual diagnostic plots. Figure 4 demonstrates the  
332 application of the web-app to the Gingera catchment on Cotter River (Australia), using GR4J pre-  
333 calibrated to the log-flow NSE ( $\lambda = 0$  and  $A^* = 0$ ).

334

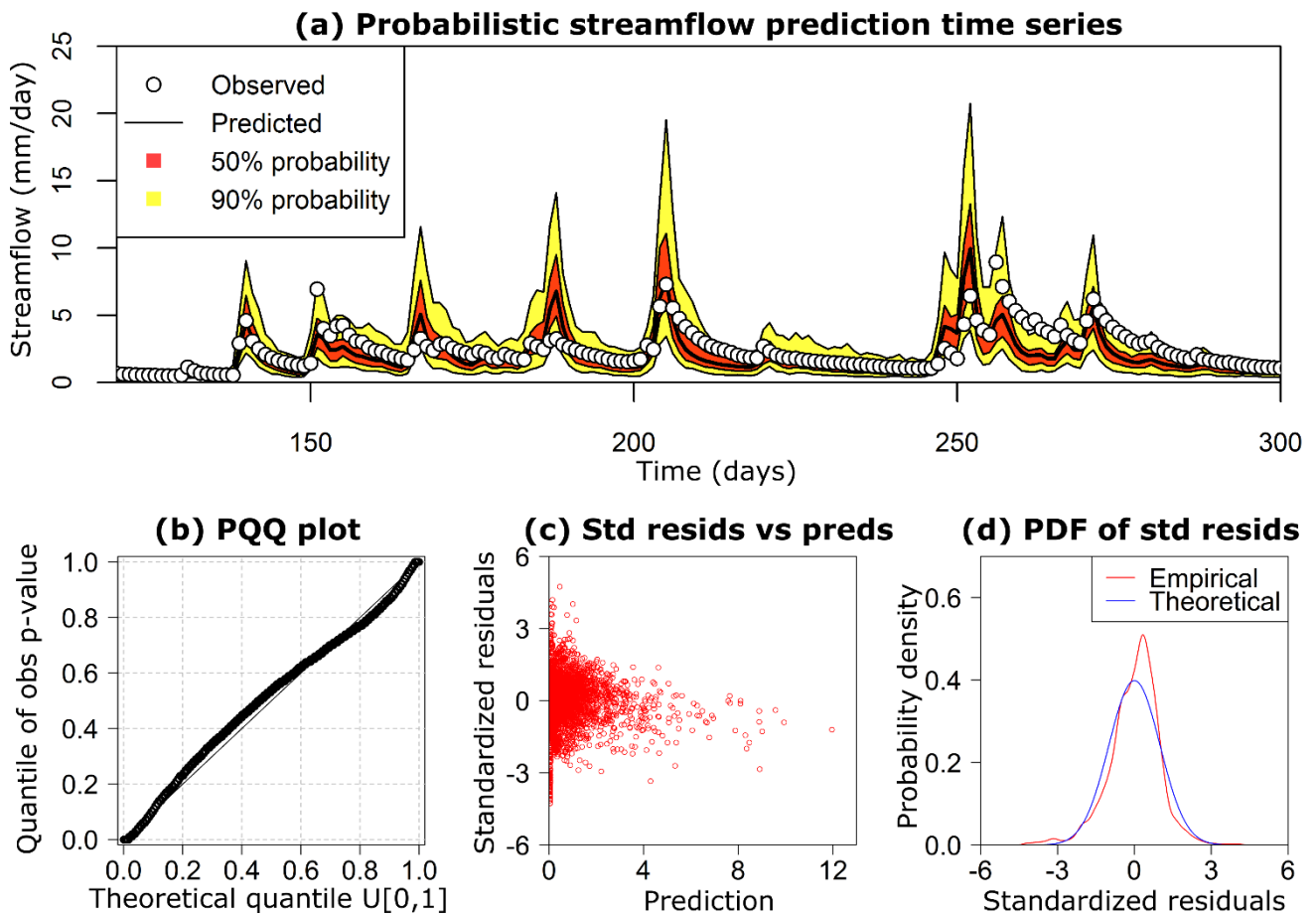


Figure 4: A selection of figures constructed from results obtained using LS-MoM approach web-app. Predictions for the Gingera catchment over the period May-October 1978 are shown, based on the GR4J model pre-calibrated to the NSE of log transformed flows. Shown are (a) 50% and 90% probability limits of the streamflow time series; (b) predictive quantile-quantile (PQQ) plot to assess the reliability of predictions; (c) residual error diagnostic plot of the dependence of standardized residuals  $\eta$  on the predicted streamflow; and (d) probability density of standardized residuals compared to the assumed error model. See Evin et al. (2013) for additional details on these diagnostics.

335

#### 336 6.4. Limitations and future work

337 Several limitations of the LS-MoM approach warrant further investigation:

- 338 1. The *a priori* fixed transformation parameters can affect performance. Guidance is available for  
339 selecting the Box-Cox parameters  $\lambda$  (McInerney et al., 2017) and  $A^*$  (Section 6.2). For other  
340 transformations, such as the log-sinh (Wang et al., 2012), less guidance might be available;
- 341 2. The LS-MoM approach may be difficult to apply to more complex non-Gaussian residual error  
342 models, including those that treat zero flows (Smith et al., 2010, Wang and Robertson, 2011), use  
343 mixture-based distributions (Schaepli et al., 2007), include skewness/kurtosis (Schoups and Vrugt,  
344 2010), etc.;

345 3. The assumption that posterior parametric uncertainty is small, while often appropriate when  
 346 parsimonious hydrological models are calibrated to long time series using simple residual error  
 347 models (Supplementary Material Section S1), might break down for more heavily parameterized  
 348 models, and/or when working with short data sets (e.g., Thyer et al., 2002). Under these scenarios,  
 349 especially if independent information is available, Bayesian approaches will be preferable. Further  
 350 analysis is recommended to clarify the range of hydrological model complexity and data length for  
 351 which posterior parametric uncertainty is sufficiently small to be ignored in practical streamflow  
 352 prediction contexts.

353 The LS-MoM approach and the web-app can be used for environmental modelling applications beyond  
 354 hydrology, whenever the residual error assumptions hold and parametric uncertainty is relatively small.  
 355 In addition, LS-MoM and the web-app can be used with environmental models calibrated using methods  
 356 other than (transformed) Least Squares objective functions, taking particular care to monitor predictive  
 357 performance metrics and residual error diagnostics because inconsistencies between the objective  
 358 function and the error model can lead to poor probabilistic predictions. These model setups are of  
 359 practical interest (Li et al., 2016) and warrant further investigation.

## 360 **7. Conclusions**

361 This study introduces a simplified approach for generating probabilistic predictions. The LS-MoM  
 362 approach uses Least Squares (LS) optimization to estimate hydrological model parameters and simple  
 363 method-of-moments (MoM) estimators of error model parameters to describe uncertainty in predictions.  
 364 It can be used in combination with many existing hydrological modelling packages, and achieves similar  
 365 predictive performance to more complicated maximum-likelihood and Bayesian approaches while  
 366 reducing computational costs by factors of two or more. A public web-app is made available to help  
 367 users apply the LS-MoM approach, and bridge the gap between deterministic and probabilistic  
 368 prediction techniques in practical hydrological applications.

## 369 **Appendix A. Generation of probabilistic predictions**

370 In both the LS-MoM and ML-ML approaches, probabilistic predictions are represented using replicates  
 371  $\mathbf{Q}^{(r)} = \{Q_t^{(r)}, t = 1, \dots, T\}$  for  $r = 1, \dots, R$ . Given parameter values  $\{\boldsymbol{\theta}_H, \boldsymbol{\theta}_Z, \boldsymbol{\theta}_\varepsilon\}$ , the  $r$ th replicate is generated  
 372 as follows:

373 1. At time step  $t$ , sample innovation  $y_t^{(r)} \leftarrow N(0, \sigma_y^2)$  and calculate residual  $\eta_t^{(r)} = \phi_\eta \eta_{t-1}^{(r)} + y_t^{(r)}$ , as per  
 374 equations (6)-(7). Note that for  $t = 1$ , we directly sample  $\eta_1^{(r)} \leftarrow N(0, \sigma_\eta^2)$ ;

375 2. Calculate replicate  $Q_t^{(r)}$  by rearranging equation (5),

$$376 \quad Q_t^{(r)} = Z^{-1}(Z(Q_t^{0_H}) + \eta_t^{(r)}) \quad (14)$$

377 3. Repeat for  $t + 1$ , etc.

378 For practical purposes,  $Q_t^{(r)}$  is truncated if it falls outside  $Q_{\min} = 0$  and  $Q_{\max} = 10 \times \max(\tilde{Q})$ .

## 379 Acknowledgments

380 This work was funded by Australian Research Council grant LP140100978 with the Australian Bureau  
 381 of Meteorology and South East Queensland Water. We thank the Associate Editor and four anonymous  
 382 reviewers for their insightful comments and suggestions. Simulations were performed on the Phoenix  
 383 cluster at the University of Adelaide. We thank Michael Leonard for hosting the web-app on his server.  
 384 Data for the Australian catchments was obtained from the Hydrologic Reference Stations database  
 385 provided by the Australian Bureau of Meteorology (<http://www.bom.gov.au/water/hrs>). The MOPEX  
 386 dataset for the USA catchments is available on request from Qingyun Duan.

## 387 References

- 388 ANDREWS, F. T., CROKE, B. F. W. & JAKEMAN, A. J. 2011. An open software environment for hydrological  
 389 model assessment and development. *Environmental Modelling & Software*, 26, 1171-1185.  
 390 BATES, B. C. & CAMPBELL, E. P. 2001. A Markov chain Monte Carlo scheme for parameter estimation and  
 391 inference in conceptual rainfall-runoff modeling. *Water Resources Research*, 37, 937-947,  
 392 doi:10.1029/2000WR900363.  
 393 BERGSTRÖM, S. 1995. The HBV model. In: SINGH, V. P. (ed.) *Computer Models of Watershed Hydrology*. Water  
 394 Resources Publications, Highlands Ranch, CO.  
 395 BOX, G. E. P. & COX, D. R. 1964. An analysis of transformations. *Journal of the Royal Statistical Society, Series B*,  
 396 26, 211-252.  
 397 BOX, G. E. P. & JENKINS, G. M. 1970. *Time series analysis: forecasting and control*, San Francisco, CA, Holden-  
 398 Day.  
 399 CHAPMAN, T. G. Optimization of a rainfall-runoff model for an arid zone catchment. I.A.S.H.-UNESCO  
 400 Symposium on the Results of Research on Representative and Experimental Basins, 1970 Wellington,  
 401 New Zealand. IASH-AISH Publ., 126-144.  
 402 CHARNES, A., FROME, E. L. & YU, P. L. 1976. The Equivalence of Generalized Least Squares and Maximum  
 403 Likelihood Estimates in the Exponential Family. *Journal of the American Statistical Association*, 71, 169-  
 404 171.  
 405 CHIEW, F. H. S., STEWARDSON, M. J. & MCMAHON, T. A. 1993. Comparison of six rainfall-runoff modelling  
 406 approaches. *Journal of Hydrology*, 147, 1-36.

- 407 CORON, L., THIREL, G., DELAIGUE, O., PERRIN, C. & ANDRÉASSIAN, V. 2017. The suite of lumped GR  
 408 hydrological models in an R package. *Environmental Modelling & Software*, 94, 166-171.
- 409 DAWDY, D. R. & LICHTY, R. 1968. Methodology of hydrologic model building. *Proceedings, use of analog and*  
 410 *digital computers in hydrology*, 2, 347-355.
- 411 DOHERTY, J. 2004. PEST—Model independent parameter estimation 5th edition. Watermark Numerical  
 412 Computing. Australia.
- 413 DUAN, Q., SCHAAKE, J., ANDREASSIAN, V., FRANKS, S. W., GOTETI, G., GUPTA, H. V., GUSEV, Y. M., HABETS, F.,  
 414 HALL, A., HAY, L., HOGUE, T., HUANG, M., LEAVESLEY, G., LIANG, X., NASONOVA, O. N., NOILHAN, J.,  
 415 OUDIN, L., SOROOSHIAN, S., WAGENER, T. & WOOD, E. F. 2006. Model Parameter Estimation  
 416 Experiment (MOPEX): An overview of science strategy and major results from the second and third  
 417 workshops. *Journal of Hydrology*, 320, 3-17.
- 418 ENGELAND, K. & STEINSLAND, I. 2014. Probabilistic postprocessing models for flow forecasts for a system of  
 419 catchments and several lead times. *Water Resources Research*, 50, 182-197.
- 420 EVIN, G., KAVETSKI, D., THYER, M. & KUCZERA, G. 2013. Pitfalls and improvements in the joint inference of  
 421 heteroscedasticity and autocorrelation in hydrological model calibration. *Water Resources Research*, In  
 422 Press, W012972, doi:10.1002/wrcr.20284.
- 423 EVIN, G., THYER, M., KAVETSKI, D., MCINERNEY, D. & KUCZERA, G. 2014. Comparison of joint versus  
 424 postprocessor approaches for hydrological uncertainty estimation accounting for error autocorrelation  
 425 and heteroscedasticity. *Water Resources Research*, 50, 2350-2375.
- 426 GAN, T. Y., DLAMINI, E. M. & BIFTY, G. F. 1997. Effects of model complexity and structure, data quality, and  
 427 objective functions on hydrologic modeling. *Journal of Hydrology*, 192, 81-103.
- 428 JOSEPH, J. F. & GUILLAUME, J. H. A. 2013. Using a parallelized MCMC algorithm in R to identify appropriate  
 429 likelihood functions for SWAT. *Environmental Modelling & Software*, 46, 292-298.
- 430 KAVETSKI, D. 2018. Parameter Estimation and Predictive Uncertainty Quantification in Hydrological Modelling.  
 431 In: DUAN, Q., PAPPENBERGER, F., THIELEN, J., WOOD, A., CLOKE, H. L. & SCHAAKE, J. C. (eds.)  
 432 *Handbook of Hydrometeorological Ensemble Forecasting*. Springer Berlin Heidelberg.
- 433 KAVETSKI, D. & CLARK, M. P. 2010. Ancient numerical demons of conceptual hydrological modeling. Part 2:  
 434 Impact of time stepping scheme on model analysis and prediction. *Water Resources Research*, 46,  
 435 W10511, doi:10.1029/2009WR008896.
- 436 KRZYSZTOFOWICZ, R. 2002. Bayesian system for probabilistic river stage forecasting. *Journal of Hydrology*, 268,  
 437 16-40.
- 438 KUCZERA, G. 1983. Improved parameter inference in catchment models: 1. Evaluating parameter uncertainty.  
 439 *Water Resources Research*, 19, 1151-1162, doi:10.1029/WR019i005p01151.
- 440 KUCZERA, G., KAVETSKI, D., FRANKS, S. & THYER, M. 2006. Towards a Bayesian total error analysis of  
 441 conceptual rainfall-runoff models: Characterising model error using storm-dependent parameters.  
 442 *Journal of Hydrology*, 331, 161-177, doi:10.1016/j.jhydrol.2006.05.010.
- 443 KUMAR, R., SAMANIEGO, L. & ATTINGER, S. 2010. The effects of spatial discretization and model  
 444 parameterization on the prediction of extreme runoff characteristics. *Journal of Hydrology*, 392, 54-69.
- 445 LI, M., WANG, Q. J., BENNETT, J. C. & ROBERTSON, D. E. 2016. Error reduction and representation in stages  
 446 (ERRIS) in hydrological modelling for ensemble streamflow forecasting. *Hydrol. Earth Syst. Sci.*, 20,  
 447 3561-3579.
- 448 LOUCKS, D. P., STEDINGER, J. R. & HAITH, D. A. 1981. *Water resource systems planning and analysis*, Prentice-  
 449 Hall.
- 450 MARTINS, E. S. & STEDINGER, J. R. 2000. Generalized maximum-likelihood generalized extreme-value quantile  
 451 estimators for hydrologic data. *Water Resources Research*, 36, 737-744.
- 452 MCINERNEY, D., THYER, M., KAVETSKI, D., LERAT, J. & KUCZERA, G. 2017. Improving probabilistic prediction of  
 453 daily streamflow by identifying Pareto optimal approaches for modeling heteroscedastic residual  
 454 errors. *Water Resources Research*.
- 455 OUDIN, L., ANDREASSIAN, V., MATHEVET, T., PERRIN, C. & MICHEL, C. 2006. Dynamic averaging of rainfall-  
 456 runoff model simulations from complementary model parameterizations. *Water Resources Research*,  
 457 42.

- 458 PERRIN, C., MICHEL, C. & ANDREASSIAN, V. 2003. Improvement of a parsimonious model for streamflow  
459 simulation. *Journal of Hydrology*, 279, 275-289, doi:10.1016/S0022-1694(03)00225-7.
- 460 PUSHPALATHA, R., PERRIN, C., MOINE, N. L. & ANDRÉASSIAN, V. 2012. A review of efficiency criteria suitable  
461 for evaluating low-flow simulations. *Journal of Hydrology*, 420, 171-182.
- 462 RENARD, B., KAVETSKI, D., LEBLOIS, E., THYER, M., KUCZERA, G. & FRANKS, S. W. 2011. Toward a reliable  
463 decomposition of predictive uncertainty in hydrological modeling: Characterizing rainfall errors using  
464 conditional simulation. *Water Resources Research*, 47, W11516, doi:10.1029/2011WR010643.
- 465 SALAS, J. D. 1993. Analysis and Modeling of Hydrologic Time Series. In: MAIDMENT, D. R. (ed.) *The McGraw Hill  
466 Handbook of Hydrology*. New York, USA: McGraw-Hill.
- 467 SCHAEFLI, B., TALAMBA, D. B. & MUSY, A. 2007. Quantifying hydrological modeling errors through a mixture of  
468 normal distributions. *Journal of Hydrology*, 332, 303-315, doi:10.1016/j.jhydrol.2006.07.005.
- 469 SCHARFFENBERG, W. A., FLEMING, M. J. & CENTER, H. E. 2006. Hydrologic Modeling System HEC-HMS: User's  
470 Manual.: US Army Corps of Engineers, Hydrologic Engineering Center.
- 471 SCHOUPS, G. & VRUGT, J. A. 2010. A formal likelihood function for parameter and predictive inference of  
472 hydrologic models with correlated, heteroscedastic and non-Gaussian errors. *Water Resources  
473 Research*, 46, W10531, doi:10.1029/2009WR008933.
- 474 SEIBERT, J. 2005. HBV light version 2, user's manual. Stockholm University.
- 475 SERVAT, E. & DEZETTER, A. 1991. Selection of calibration objective functions in the context of rainfall-runoff  
476 modelling in a Sudanese savannah area. *Hydrological Sciences Journal*, 36, 307-330.
- 477 SMITH, T., SHARMA, A., MARSHALL, L., MEHROTRA, R. & SISSON, S. 2010. Development of a formal likelihood  
478 function for improved Bayesian inference of ephemeral catchments. *Water Resources Research*, 46,  
479 W12551, doi:10.1029/2010WR009514.
- 480 SOROOSHIAN, S. & DRACUP, J. A. 1980. Stochastic parameter estimation procedures for hydrological rainfall-  
481 runoff models: Correlated and heteroscedastic error cases. *Water Resources Research*, 16, 430-442,  
482 doi:10.1029/WR016i002p00430.
- 483 SUN, R., YUAN, H. & LIU, X. 2017. Effect of heteroscedasticity treatment in residual error models on model  
484 calibration and prediction uncertainty estimation. *Journal of Hydrology*.
- 485 THYER, M., KUCZERA, G. & WANG, Q. J. 2002. Quantifying parameter uncertainty in stochastic models using  
486 the Box-Cox transformation. *Journal of Hydrology*, 265, 246-257, doi:10.1016/S0022-1694(02)00113-0.
- 487 TONKIN, M. & DOHERTY, J. 2009. Calibration-constrained Monte Carlo analysis of highly parameterized models  
488 using subspace techniques. *Water Resources Research*, 45.
- 489 VAZE, J., JORDAN, P., BEECHAM, R., FROST, A. & SUMMERELL, G. 2012. Guidelines for rainfall-runoff modelling.  
490 VOGEL, R. M. 2017. Stochastic watershed models for hydrologic risk management. *Water Security*, 1, 28-35.
- 491 VRUGT, J. A., TER BRAAK, C. J. F., DIKS, C. G. H., ROBINSON, B. A., HYMAN, J. M. & HIGDON, D. 2009.  
492 Accelerating Markov Chain Monte Carlo Simulation by Differential Evolution with Self-Adaptive  
493 Randomized Subspace Sampling. *International Journal of Nonlinear Sciences and Numerical Simulation*,  
494 10, 273-290.
- 495 WANG, Q. J. & ROBERTSON, D. E. 2011. Multisite probabilistic forecasting of seasonal flows for streams with  
496 zero value occurrences. *Water Resources Research*, 47.
- 497 WANG, Q. J., SHRESTHA, D. L., ROBERTSON, D. E. & POKHREL, P. 2012. A log-sinh transformation for data  
498 normalization and variance stabilization. *Water Resources Research*, 48.
- 499 WELSH, W. D., VAZE, J., DUTTA, D., RASSAM, D., RAHMAN, J. M., JOLLY, I. D., WALLBRINK, P., PODGER, G. M.,  
500 BETHUNE, M., HARDY, M. J., TENG, J. & LERAT, J. 2013. An integrated modelling framework for  
501 regulated river systems. *Environmental Modelling & Software*, 39, 81-102.
- 502 YANG, J., REICHERT, P., ABBASPOUR, K. C. & YANG, H. 2007. Hydrological modelling of the chaohe basin in  
503 china: Statistical model formulation and Bayesian inference. *Journal of Hydrology*, 340, 167-182.
- 504 YE, W., JAKEMAN, A. J. & YOUNG, P. C. 1998. Identification of improved rainfall-runoff models for an  
505 ephemeral low-yielding Australian catchment. *Environmental Modelling & Software*, 13, 59-74.